Molecular Therapy
Nucleic Acids
Original Article

Hepatocellular carcinoma progression mediated by hepatitis B virus-encoded circRNA HBV_circ_1 through interaction with CDK1

Min Zhu,[1,2] Zi Liang,[1,2] Jun Pan,[1,2] Xing Zhang,[1] Renyu Xue,[1] Guangli Cao,[1] Xiaolong Hu,[1] and Chengliang Gong[1]

[1]School of Biology & Basic Medical Science, Soochow University, Suzhou 215123, China

Hepatitis B virus (HBV) produces circular RNA (circRNA), whose functions have not yet been clearly elucidated. In this study, a novel circRNA HBV_circ_1 produced by HBV was identified in HBV-positive HepG2.2.15 cells and HBV-related hepatocellular carcinoma (HCC) tissue (HCCT). Microarray analysis of 68 HCCT samples showed that HBV_circ_1 abundance was significantly higher than that in paracancerous tissues. In addition, survival rate of HBV_circ_1-positive patients was significantly lower compared with HBV_circ_1-negative patients. Transient expression indicated that HBV_circ_1 enhanced cell proliferation, migration, and invasion and inhibited apoptosis *in vitro*. Furthermore, ectopical HBV_circ_1 expression increased tumor size *in vivo*. HBV_circ_1 was confirmed to interact with cyclin-dependent kinase 1 (CDK1) to regulate cell proliferation. These results suggest that HCC progression may be promoted by interaction of HBV_circ_1 with CDK1. Our data not only showed a novel clue to understand carcinogenesis and progress of HBV-related HCC but also provided a new target for the development of therapeutic drugs.

INTRODUCTION

Approximately 2 billion people worldwide are currently infected by hepatitis B virus (HBV), of whom about 350 million people are chronically infected with HBV and remain at a high risk of developing liver cirrhosis and hepatic cellular cancer (HCC).[1,2] Therefore, HBV infection represents a major global public health challenge. HBV is a small DNA virus of the *Hepadnaviridae* family, whose genetic material is circular and partially double-stranded DNA that is only 3.2 kb in size. After invading the host cell nucleus, the HBV genomic DNA is converted into a covalently closed circular DNA (cccDNA) that accumulates in the nucleus as a stable episome organized into nucleosomal structures.[3] cccDNA functions as a minichromosome, which is responsible for the persistence of HBV infection. It also constitutes the template for viral mRNA transcription, including 2.4 kb and 2.1 kb RNAs encoding different forms of hepatitis B surface antigen proteins (HBsAg), a 0.7 kb HBx RNA that encodes HBx protein, and two RNAs longer than the genome length (3.5 kb, 3.6 kb), known as pgRNA and precore RNA (pcRNA).[4] pgRNA is the template for viral polymerase (pol) and core protein (HBc) translation, which is reverse transcribed into relaxed circular double-stranded DNA (rcDNA).[5] pcRNA is longer than pgRNA and directs the synthesis of precore (preC) protein, a precursor of the hepatitis B e antigen (HBeAg).[6]

HBV infection is a key risk factor for chronic hepatitis, liver cirrhosis, and HCC. The mechanism of carcinogenesis and progress of HBV-related HCC has been extensively studied.[7–11] HBV contributes to HCC development through direct and indirect mechanisms. Its DNA is integrated in the host genome, which may precede clonal tumor expansion and induce genomic instability, as well as direct insertional mutagenesis, eventually leading to HCC.[12,13] Prolonged expression of viral proteins, including HBx and large-envelope protein, constitutes carcinogenic factors that may regulate cell death, proliferation, and signaling pathways.[14–16] Moreover, HBx and HBc proteins induce epigenetic modifications targeting the expression of tumor-suppressor genes to promote HCC development.[17,18] HBV contributes to HCC by reactivation of telomerase activity through HBx expression.[19]

An increasing number of studies indicate that HBV modulates different host microRNAs (miRNAs) and long non-coding RNAs (lncRNAs), particularly through the HBx protein. Deregulation of miRNAs, such as miR-222, miR-25, miR-92a, miR-1, let-7f, and miR-21, is associated with different stages of HCC.[20–22] Dysregulated lncRNAs have been also identified in HBV-related HCC. Growing evidence has shown that lncRNAs function in HCC progression and play essential roles in modulation of cell proliferation, apoptosis, invasion, metastasis, and autophagy.[23]

HBV RNAs mainly template for viral proteins and viral DNAs, but increasing evidence indicates that HBV RNAs may act as host miRNAs sponges to upregulate miRNA target expression, possibly resulting in diverse pathologies.[24] Moreover, it was reported that viral

Received 18 December 2020; accepted 10 August 2021;
https://doi.org/10.1016/j.omtn.2021.08.011.

[2]These authors contributed equally

Correspondence: Xiaolong Hu, School of Biology & Basic Medical Science, Soochow University, Suzhou 215123, China.
E-mail: xlhu2013@suda.edu.cn
Correspondence: Chengliang Gong, School of Biology & Basic Medical Science, Soochow University, Suzhou 215123, China.
E-mail: gongcl@suda.edu.cn

Please cite this article in press as: Zhu et al., Hepatocellular carcinoma progression mediated by hepatitis B virus-encoded circRNA HBV_circ_1 through interaction with CDK1, Molecular Therapy: Nucleic Acids (2021), https://doi.org/10.1016/j.omtn.2021.08.011

replication is promoted via sequestering cellular miRNAs, such as miR-122 and miR-15 family, by HBV RNAs.[25]

Previous studies have shown that HBV encodes miRNAs, HBV-miR-2, and HBV-miR-3. HBV-miR-2 promotes oncogenic activity by suppressing tripartite motif containing 35 expression and enhancing ras-related nuclear protein expression in liver cancer cells,[26] whereas HBV-miR-3 targets the HBV 3.5-kb transcript to reduce HBc and pgRNA levels, which results in attenuation of HBV replication.[27]

As mentioned above, HBV contributes to HCC development by its DNA, RNA (pcRNA, pgRNA, mRNAs, and miRNA), and viral proteins by direct and indirect mechanisms. HBV may also generate novel molecules that play important roles in HCC progression. Circular RNAs (circRNAs) are a type of closed circular RNAs produced by back splicing. circRNAs have been found in archaea, yeast, plants, invertebrates, and vertebrates. Increasing evidence indicates that circRNAs have multiple biological functions, including regulation of transcription and splicing, sponging miRNAs and proteins, and serving as translation templates.[28,29] In addition to cellular circRNAs, it has been reported that gammaherpesviruses, including Epstein-Barr virus (EBV), Rhesus lymphocryptovirus (rLCV), Kaposi's sarcoma herpesvirus (KSHV), and murine herpesvirus 68 (MHV68) produce circRNAs.[30–34]

A systematic survey of 11,924 circRNAs from 23 viral species was developed by computational prediction, using viral-infection-related RNA sequencing data. Results suggested that some single-stranded RNA viruses and retro-transcribing viruses, such as Zika virus, influenza A virus, Zaire ebolavirus, and human immunodeficiency virus, may also generate viral circRNAs.[35] Recently, a circRNA derived from HBV pgRNA was identified.[36] Moreover, 5 circRNAs encoded by HBV were also identified, using viral-infection-related RNA sequencing data.[35] However, the biological functions of circRNA encoded by HBV are still unknown.

In the present study, a novel circRNA HBV_circ_1 encoded by HBV was found in HBV-positive HepG2.2.15 cells and HBV-related HCC tissue (HCCT). We showed that HBV_circ_1 enhanced cell proliferation, migration, and invasion; inhibited apoptosis *in vitro*; increased tumor size *in vivo*; and interacted with cyclin-dependent kinase 1 (CDK1). This suggests that HCC progression may be promoted by interaction of HBV_circ_1 with CDK1. Our findings provide a novel clue to understand HBV hepatocarcinogenesis and a new target for the development of therapeutic drugs for HBV-related HCC.

RESULTS

HBV_circ_1 with two junction sites derives from pgRNA/pcRNA

We previously performed RNA sequencing with the HBV-positive cell line HepG2.2.15, using poly(A)$^+$-selected or RNase R-treated RNA libraries (accession numbers SRR7812043-SRR7812048 and SRR7892713-SRR7892718). Sequencing results showed that a candidate circRNA termed HBV_circ_1 (2,497 bp in size) mapped to the 489–2,985 nucleotide (nt) region of the HBV genome (GenBank: KU668446.1).

HBV transcription began from different transcriptional start sites on the HBV cccDNA but ended at a common transcription termination signal. It is known that 2.4 kb, 2.1 kb, 0.7 kb, and 3.5–3.6 kb RNAs are transcribed from HBV cccDNA.[5,6] Furthermore, 2.4 kb, 2.1 kb, and 0.7 kb viral RNAs, but not HBV_circ_1, have the whole or partial sequence of 2,986–488 nt region corresponding to the HBV genome. Therefore, HBV_circ_1 is not generated from 2.4 kb, 2.1 kb, and 0.7 kb HBV RNAs. Sequence alignment showed that the HBV_circ_1 sequence consisted of two parts derived from pgRNA/pcRNA, one of which corresponds to the 489–1,932 nt region and the other one to the 1,933–2,985 nt region of the HBV genome. As shown in Figure 1A, after the sequence corresponding to HBV genome 2,986–488 nt region was removed from pgRNA/pcRNA, the remaining pgRNA/pcRNA sequences formed a junction site (junction site B; Figure 1A). In particular, the dinucleotides at the first two and last two positions of the deleted HBV pgRNA sequence were GU and AG, respectively, which agreed with the intron conserved boundary sequences (Figure 1A).

Sequence analysis showed that the 113-base sequence (corresponding to the region 1,820–1,932 nt of the HBV genome) located at the 5′ terminal region of pgRNA/pcRNA was directly repeated with the 3′ terminal sequence of pgRNA/pcRNA. After removing the non-repeating sequence located at the 5′ and 3′ terminals and one of the repeating units, the two ends of pgRNA/pcRNA formed another junction site (junction site A), thus evidencing that HBV_circ_1 possesses two junction sites.

Reverse transcription introduces template-switching artifacts, and RNase R does not digest all linear RNAs and stall in the middle of transcripts.[37] Therefore, some circRNAs predicted by different computational pipelines might be an artifact.[38] To confirm that HBV_circ_1 was not a sequencing artifact or noise, RT-PCR was performed with the divergent primers Q-HBV_circ_1-Forward/Q-HBV_circ_1-Reverse (Table 1), after the extracted RNA from HBV-positive HepG2.2.15 cells was treated with DNase I and RNase R. Results showed that the PCR product representing HBV_circ_1 was amplified from the RNA samples. Sanger sequencing of the PCR product yielded the same spliced junction site B as high-throughput sequencing (Figure 1B). The expected results were also obtained using a similar approach to confirm junction site A (Figure 1C). Moreover, specific signal bands were observed by northern blotting with the probe targeting junction B in HBV-positive HepG2.2.15 cells, but not in HBV-negative HepG 2 cells, whether the samples were treated with RNase R or not (Figure 1D). Furthermore, Primer2-Forward and Primer3-Reverse crossing junction site A and Primer2-Reverse and Primer3-Forward crossing junction site B were used for PCR amplification to characterize the full sequence of HBV_circ_1. Specific PCR products were obtained from HBV-positive HepG2.2.15 cell RNA, but not from HBV-negative HepG2 cell RNA, indicating that junction sites A and B were on the same molecule. The recovered PCR product was further cloned into the T vector.

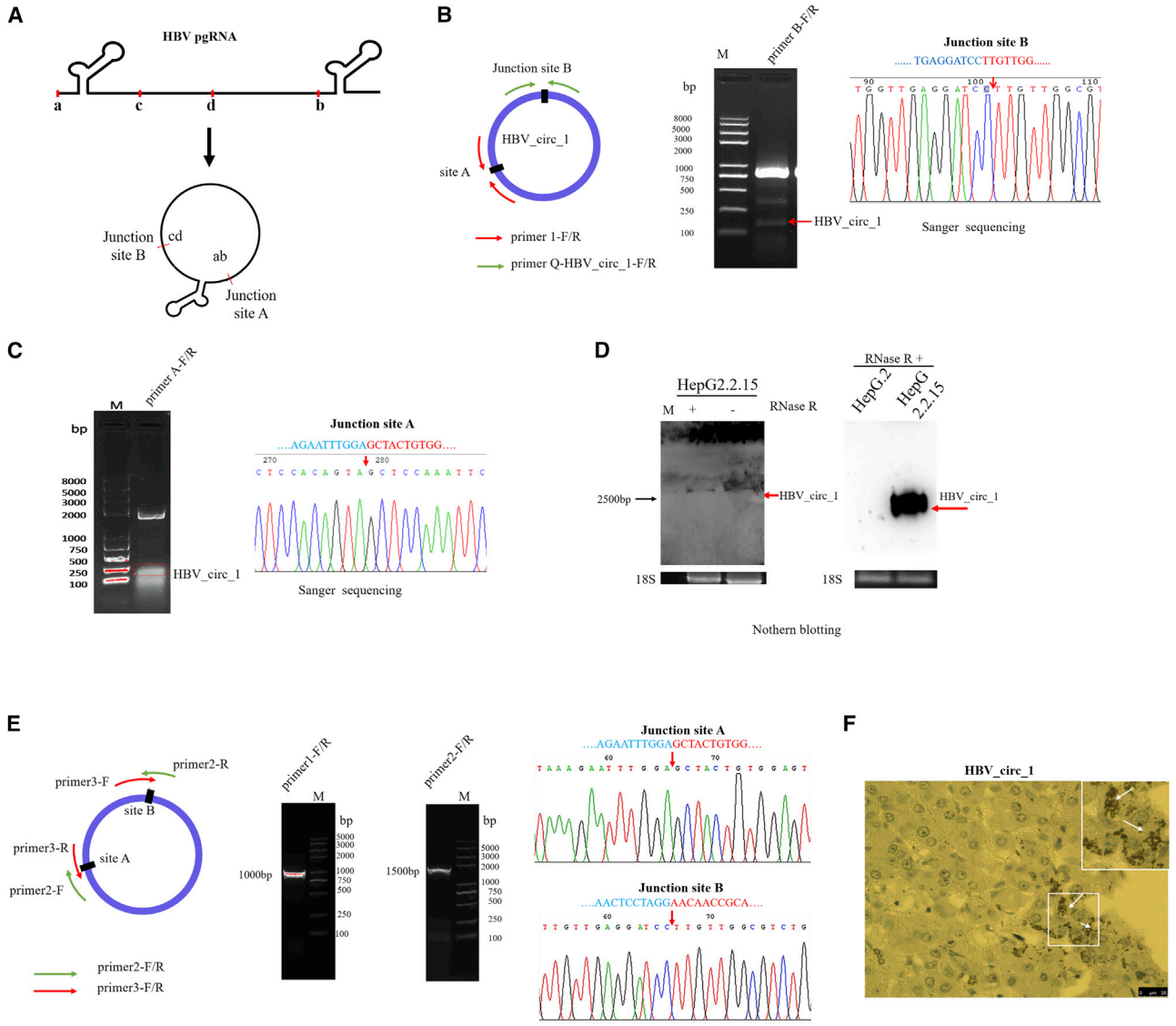

Figure 1. Validation of full-length HBV_circ_1

(A) Formation mechanism of HBV_circ_1. (B) RT-PCR and Sanger sequencing validation of HBV_circ_1 at junction B. (C) RT-PCR and Sanger sequencing validation of HBV_circ_1 at junction A. (D) Northern blotting validation of HBV_circ_1. 18S represents 18S rRNA, as the internal control. (E) RT-PCR and Sanger sequencing validation of full-length HBV_circ_1. Left: the diagram of primers crossing junction site A and junction site B. Middle: the electrophoresis RT-PCR products. Right: Sanger sequencing of RT-PCR products. Red arrow represents HBV_circ_1 junction site. (F) Representative image of HBV_circ_1 in tumor tissue with hybridization *in situ*.

HBV_circ_1 sequence, as determined by Sanger sequencing, agreed with the results obtained by RNA_Seq (Figure 1E). These results indicated that HBV_circ_1 with two junction sites derived from pgRNA/pcRNA and was present in the HBV-positive HepG 2.2.15 cells. To confirm that HBV_circ_1 is generated *in vivo*, hybridization *in situ* experiments were conducted, using tissue microarrays. Results showed that HBV_circ_1 was detected in HBV-positive tissues, and HBV_circ_1 was mainly located in the cytoplasm (Figure 1F). These results strongly suggested that HBV_circ_1 is produced *in vivo*.

Expression level of HBV_circ_1 in HCCT

To evaluate whether HBV_circ_1 expression level was associated with the HBV-related HCCT, we evaluated its expression in clinical samples by *in situ* hybridization in 68 HCCT samples and paired with paracancerous tissue (HCCPT), using microarrays. Statistical results showed that the expression level was significantly higher than that in HCCPT (Figures 2A and 2B). In addition, we found that the survival rate of HBV_circ_1-positive patients was significantly lower than that of HBV_circ_1-negative patients (Figure 2C). These results suggested that HBV_circ_1 was involved in HCC.

Please cite this article in press as: Zhu et al., Hepatocellular carcinoma progression mediated by hepatitis B virus-encoded circRNA HBV_circ_1 through interaction with CDK1, Molecular Therapy: Nucleic Acids (2021), https://doi.org/10.1016/j.omtn.2021.08.011

Table 1. Primers and probe sequences used in this manuscript

Gene name	Forward (5′→3′)	Reverse (5′→3′)
Q-HBV_circ_1	TTGAGCAGTAGTCATGCAGG	GATTCTTTCCCGACCACC
Primer 1	ACAGAGCTGAGGCGGTATCT	GAGGAGTTGGGGGAGGAGAT
Primer 2	TTATAAAGAATTTGGAGCTA	CTGGTTGTTGAGGATCCTTG
Primer 3	GCCAGACGCCAACAAGGATC	GTAACTCCACAGTAGCTCCA
β-actin	CTCCATCCTGGCCTCGCTGT	GCTGTCACCTTCACCGTTCC
CDK1	AAAATTGGAGAAGGTACCTATGGA	CCCTTCCTCTTCACTTTCTAGTCTG
pLCDH-HBV_circ_1	GAATTCTGAAATATGCTATCTT ACAGGATCCTCA ACAACCAGCACG)	GGATCCTCAAGAAAAAATATATTACC TTGTTGGCGTCTGGCCAGG
T7-circ_gfp	TAATACGACTCACTATAGGCAAGCT GACCCTGAAGTTC	GTAGTTGTACTCCAGCTTGTG
T7-HBV_circ_1	TAATACGACTCACTATAGGCAAG CTGACCCTGAAGTTC	CTTGTTGGCGTCTGGCCAGG
HBV_circ_1 probe	5′Biotion- GTGGTTGAGGATCCTT GTTGGCGTCTG	
HBV_circ_1 probe-A	TTGAGCAGTAGTCATGCAGGTCCGG CATGGTCCCGTGCTGGTGGTTGAGG ATCCTTGTTGGCGTCTGGCCAGGTG TCCTTGTTGGGATTGAAGTCCCAAT CTGGATTTGCTGTGTTTGCTCTGAA GGCTGGATCCAACTGGTGGTCGGG AAAGAATC	

HBV_circ_1 stimulates cell proliferation, migration, and invasion and inhibits apoptosis *in vitro*

The liver cancer cell lines HepG2 and SMMC-7721 and the normal liver cell line AML-12 were used to assess the effect of HBV_circ_1 on cell proliferation by the MTT reduction assay. Results showed that transient expression of HBV_circ_1 induced cell proliferation (Figure 3A). In the HBV_circ_1 transient expression group, the proportion of HepG2, SMMC-7721, and AML-12 cells detected in the G1 phase was 47.74%, 60.6%, and 38.1%, respectively, whereas that in the control group was 52.75%, 63.84%, and 47.7%, respectively. The proportion of HepG2, SMMC-7721, and AML-12 cells in G2/S phase increased (Figure 3B), suggesting that the cell cycle was accelerated.

Furthermore, flow cytometric analysis was conducted to detect the effect of HBV_circ_1 on apoptosis. Results showed that early apoptosis of HepG2 and AML-12 cells was inhibited by transient expression of HBV_circ_1, compared with that in the control cells (Figure 3C). As shown in Figure 3C, the percentage of early apoptotic HepG 2 cells was 1.79% in the transiently expressing HBV_circ_1 group and 11.02% in the control group. However, the apoptosis of AML-12 cells was not significantly affected by HBV_circ_1. These data demonstrated that HBV_circ_1 inhibited early apoptosis of HepG2 cells. Additionally, the Boyden chamber and migration through a polycarbonate membrane showed that HBV_circ_1 promoted cell migration and cell invasion in HepG2 and AML-12 cells (Figure 3D).

HBV_circ_1 promotes tumor size *in vivo*

To further explore the role of HBV_circ_1 in tumorigenesis *in vivo*, SMMC-7721 cells transfected with pLCDH-HBV_circ_1 or pLCDH null vector were injected into the dorsal sides of BALB/c nude mice. At 6 weeks post-inoculation, we euthanized the animals and surgically resected the subcutaneous tumor. As expected, tumor in the pLCDH-HBV_circ_1-transfected group grew faster than that in the group transfected with pLCDH null (Figures 4A–4C). Moreover, HBV_circ_1 was detected in the formed tumor by PCR and Sanger sequencing (data not shown). H&E staining was further performed to determine the effects of HBV_circ_1 on tumor development. Tumor cells with HBV_circ_1 transient expression had abnormal structure and disordered arrangement. The degree of tumor malignancy was increased compared with the control group (Figure 4D).

Nuclear protein Ki67 is widely used as a proliferation marker for tumor cell proliferation and growth,[39] whereas cyclin D1 regulates the G1/S phase transition in tumorigenesis.[40] To assess the role of HBV_circ_1 in promoting cell proliferation and cell cycle, the expression levels of Ki67 and cyclin D1 in tumor tissues were determined by immunohistochemistry. Results showed that their expression increased compared with the control group (Figure 4D), indicating that tumor size was promoted by HBV_circ_1.

HBV_circ_1 interacts with the CDK1 protein

To explore whether the cell cycle was regulated by interaction of HBV_circ_1 with proteins, RNA pull-down was conducted with biotinylated HBV_circ_1 and biotinylated circular green fluorescent protein gene sequence (circ_gfp), following the process shown in Figure 5A. The obtained precipitation complex was separated by SDS polyacrylamide gel electrophoresis (SDS-PAGE), and a specific protein band was observed in the precipitate complex of biotinylated

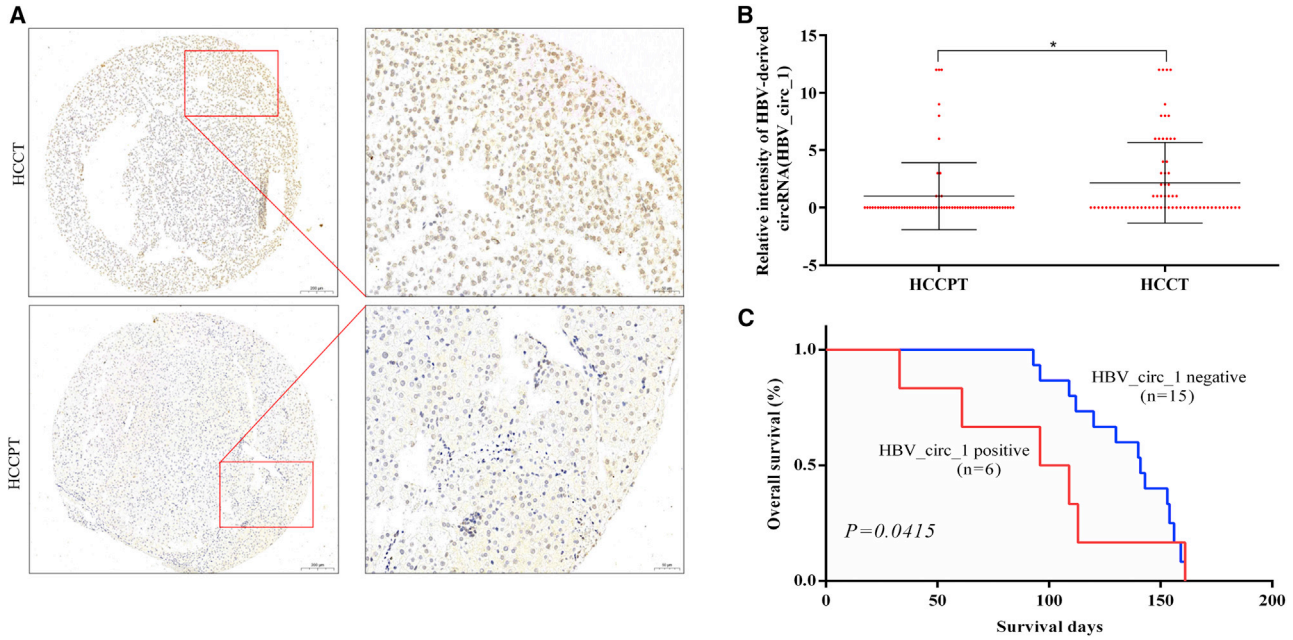

Figure 2. The expression level of HBV_circ_1 in HCC tissues was higher than that in paracancerous tissues

(A) Representative images of HBV_circ_1 *in situ* hybridization in HCC and paracancerous tissue microarray. (B) Statistics of *in situ* hybridization result in hepatocellular carcinoma and paracancerous (n = 68) tissue microarray (*p value $\leq$ 0.05). (C) Positive expression of HBV_circ_1was correlated with worse overall survival in patients with cancer (p value = 0.0415).

HBV_circ_1 compared with that of circ_gfp (Figure 5B). The protein band was recovered for identification using mass spectrometry, and 13 proteins, including CDK1, CDK18, prohibitin (PHB), and splicing factor U2AF35 kDa subunit, were identified (Table 2). CDK1 and CDK18 proteins were associated with the cell cycle.

To further verify the proteins interacted with HBV_circ_1, RNA immunoprecipitation (RIP) was conducted with the CDK1 antibody. The precipitated complex was used to extract RNA, and after the RNA was reverse transcribed into cDNA, PCR was conducted to determine the HBV_circ_1 level. Results showed that CDK1 antibody enriched higher levels of HBV_circ_1 compared with the control sample (Figure 5C). The same strategy was used to evaluate the level of HBV_circ_1 enriched by PHB and U2AF35. Results showed that HBV_circ_1 was enriched by PHB and U2AF35, achieving HBV_circ_1-interacting proteins obtained by RNA pull-down. Cell immunofluorescence experiments showed that HBV_circ_1 and CDK1 were co-localized in the nucleus (Figure 5D). Moreover, CDK1 was detected in the precipitation complex obtained by RNA pull-down with HBV_circ_1 by western blotting (Figure 5E), which further confirmed that HBV_circ_1 interacted with CDK1 protein. However, does HBV_circ_1 bind to CDK1 directly or indirectly? We expressed CDK1 recombinant proteins utilizing *E. coli* and purified CDK1 recombinant proteins for electrophoretic mobility shift assay (EMSA) and RIP *in vitro*. The RIP *in vitro* results showed that CDK1 antibody could enriched HBV_circ_1 (Figure 5F). The results of EMSA also showed that recombined CDK1 protein bound to HBV_circ_1 (Figure 5G), suggesting that HBV_circ_1 directly binds to CDK1. Therefore, we speculated that the cell phenotypic characteristics might be regulated by HBV_circ_1 via binding to CDK1.

HBV_circ_1 stimulates cell proliferation, migration, and invasion and inhibits apoptosis by binding to CDK1

In this study, we predicted the binding sites of CDK1 and HBV_circ_1 using the website http://s.tartaglialab.com/page/catrapid_group, and then we constructed HBV_circ_1-mut with deletion of CDK1 and HBV_circ_1 binding site according to the predicted outcome data. To demonstrate that HBV_circ_1 regulates cell phenotypic characteristics by binding to CDK1, the liver cancer cell line HepG2 and normal liver cell line AML-12 were used to assess the effect of HBV_circ_1 or HBV_circ_1-mut on cell proliferation by the MTT reduction assay. Results showed that compared with HBV_circ_1, cell proliferation in the HBV_circ_1-mut group reduced (Figure 6A). In addition, we found that the effect of HBV_circ_1 on cell proliferation was weakened when CDK1 was silenced (Figure 6A). Cell cycle experiments showed that the proportion of AML-12 cells detected in the G1 phase was 56.25% in the HBV_circ_1-mut transient expression group and 39.62% in slicing CDK1 group, respectively, whereas that in the HBV_circ_1 group it was 39.27%. The proportion of AML-12 cells in G2/S phase reduced (Figure 6B), suggesting that the cell cycle was slowed down when HBV_circ_1 could not bind to CDK1. However, flow cytometric analysis results showed that compared with HBV_circ_1, early apoptosis of AML-12 cells was increased slightly by transient expression of

Please cite this article in press as: Zhu et al., Hepatocellular carcinoma progression mediated by hepatitis B virus-encoded circRNA HBV_circ_1 through interaction with CDK1, Molecular Therapy: Nucleic Acids (2021), https://doi.org/10.1016/j.omtn.2021.08.011

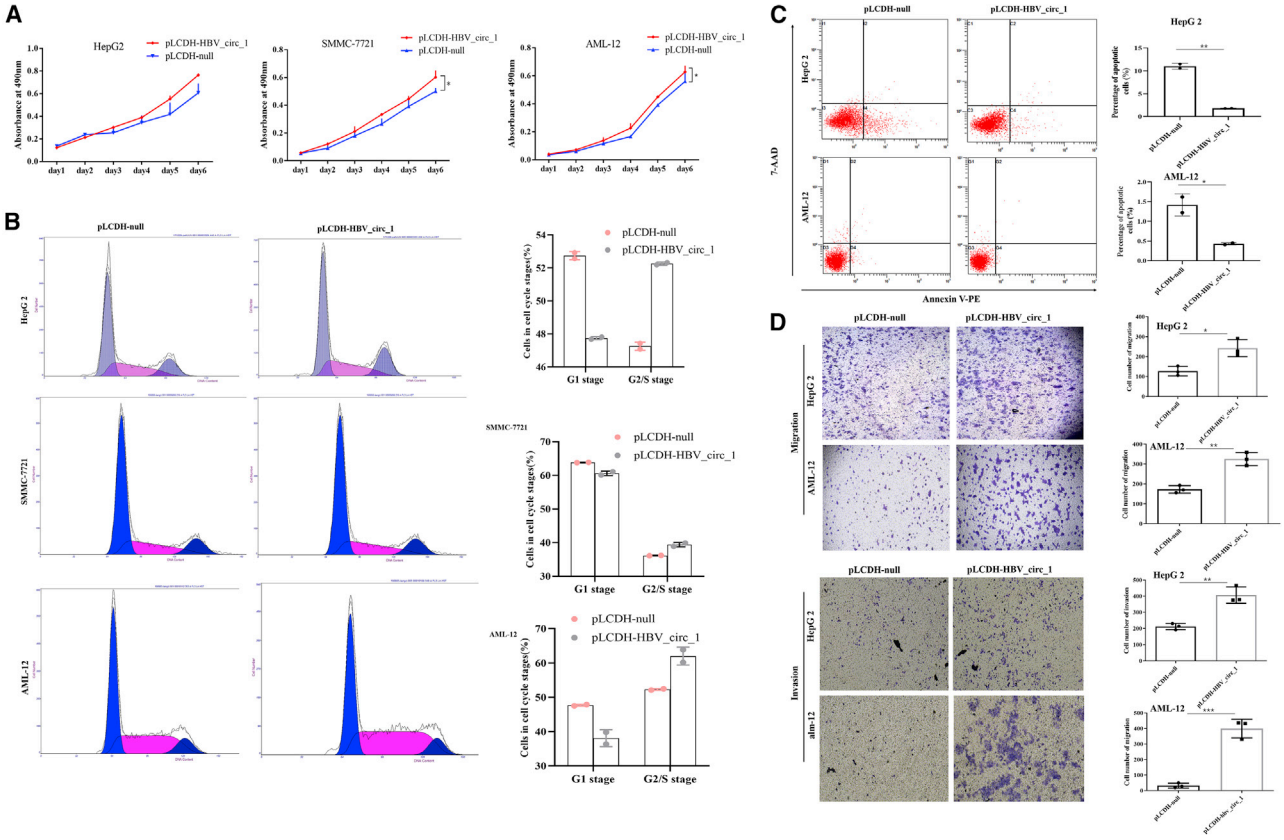

Figure 3. HBV_circ_1 promoted cell proliferation, cell cycle process, migration, and invasion and inhibited apoptosis in *vitro*

(A) Cell proliferation of pLCDH-HBV_circ_1- and pLCDH-transformed cells (HepG2, SMMC-7721, AML-12 cell line) were determined by MTT assay. (B) Cell cycle of HepG2-pLCDH-HBV_circ_1- and HepG2-pLCDH-transformed cells were determined by flow cytometry. Results of fluorescence-activated cell sorting (FACS) analysis were presented as the percentage of total cells. (C) Flow cytometry was used to detect the apoptosis of HepG2-pLCDH-HBV_circ_1- and HepG2-pLCDH-transformed cells. (D) The Transwell migration and invasion assays of HepG2-pLCDH-HBV_circ_1- and HepG2-pLCDH-transformed cells. All tests were performed at least twice (***p value $\leq$ 0.001, **p value $\leq$ 0.005, *p value $\leq$ 0.05).

HBV_circ_1-mut and by slicing CDK1 (Figure 6C). The Boyden chamber and migration through a polycarbonate membrane also showed that the effects of HBV_circ_1 on promoting cell migration and cell invasion were weakened in HepG2 and AML-12 cells by transient expression of HBV_circ_1-mut and by slicing CDK1 (Figure 6D). All of these results indicated that HBV_circ_1 promoted cell proliferation, migration, and invasion and inhibited apoptosis by binding to CDK1.

HBV_circ_1 increases CDK1 expression level

Abnormal expression of cyclin and CDKs causes cell cycle disorders, leading to uncontrolled cell proliferation and eventually carcinogenesis. CDK1 is a protein kinase that binds to cyclin and activates cell cycle progression. It is also a key player in driving the M-phase in both meiosis and mitosis.[41] We further performed real-time PCR and western blot to determine whether HBV_circ_1 alters CDK1 expression level. As shown in Figures 7A–7C, CDK1 expression significantly increased in cells transiently expressing HBV_circ-1. Moreover, CDK1 expression level in tumor with HBV_circ_1 transient expression significantly augmented compared with the control group, as measured by immunohistochemistry (Figure 7D), which indicated that HBV_circ_1 increases CDK1 expression *in vitro* and *in vivo*. Further, the Boyden chamber and migration through a polycarbonate membrane showed that cell migration and cell invasion were inhibited in HepG2 cells and AML-12 cells by slicing CDK1. However, transiently expressing HBV_circ_1 could rescue the migration and invasion of HepG2 and AML-12 cells (Figure 6D), suggesting that HBV_circ_1 may modulate cellular phenotypic characteristics by altering CDK1 expression levels.

DISCUSSION

Increasing data have shown that a variety of organisms generate circRNAs by back-splicing, including *Drosophila*,[42] rice,[43] silkworm,[44] zebrafish,[45] and humans.[46] In addition to cellular transcripts, some transcripts of gammaherpesviruses are spliced to form circRNAs.[30,31] In KSHV and EBV, some of the viral circRNAs are entirely derived from exons of the viral mRNA, and some retain introns, which are similarly formed as cellular transcripts, through back-splicing. A

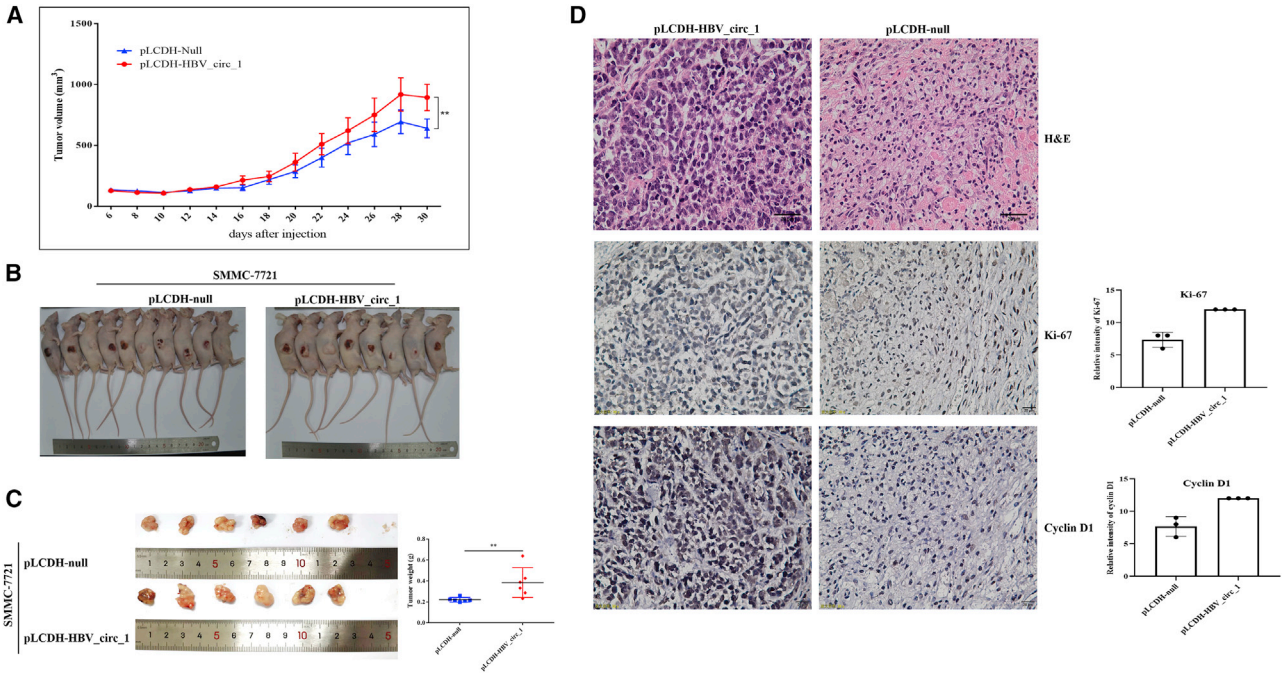

Figure 4. HBV_circ_1 promoted tumor formation in *vivo*

(A) Volume of subcutaneous xenograft tumors of SMMC-7721 cells isolated from nude mice. (B) Representative images of xenografts formed by subcutaneous injection of SMMC-7721 cells transfected with pLCDH-HBV_circ_1 or pLCDH vector into the dorsal flanks of BALB/c nude mice. (C) Representative images of the isolated tumors from injected mice. Right: Tumor weight was calculated according to the formula provided in the Materials and methods section. (D) The xenograft tumors of SMMC-7721 cells were stained by H&E. Moreover, immunohistochemistry analyses were performed to examine the expression levels of Ki67 and Cyclin D1 in xenograft tumors of SMMC-7721 cells isolated from nude mice. Left: Representative images of immunohistochemistry for Ki67 and Cyclin D1. Right: Quantitative analysis of immunohistochemistry (**p value $\leq$ 0.005, *p value $\leq$ 0.05).

previous study reported that HBV pgRNA, rather than mRNA, also forms circRNA with a size similar to that of pgRNA.[36] Five circRNAs, whose sequences corresponded the regions 282–2,985 nt, 489–2,447 nt, 489–2,985 nt, 505–2,471 nt, and 489–2,471 nt of the viral genome (GenBank: AB267090.1) encoded by HBV were identified based on HepaRG cell RNA sequencing data.[35] However, the biogenesis and function of HBV-encoded circRNAs have not been determined.

Since scrambled junctions may be formed by non-canonical splicing (i.e., *trans*-splicing), sequencing artifacts or noise might be generated by the reverse transcriptase (template-switching), and linear RNAs cannot been completely digested by RNase R.[38] Therefore, in the present study, a pgRNA/pcRNA-derived HBV_circ_1, whose sequence corresponded to the 489–2,985 nt region of the HBV genome, was validated by RT-PCR, Sanger sequencing, and northern blotting. According to the sequence and size of circRNA, we suggested that the viral circRNA confirmed by Sekiba et al.[36] and five viral circRNAs identified by Cai et al.[35] were generated from pgRNA/pcRNA, like HBV_circ_1.

Previous studies showed that in most eukaryotes, circRNAs are produced by back-splicing via the spliceosome.[47] HBV pgRNA is spliced to generate pgRNA splicing variant by removing introns from heterogeneous nuclear RNA.[48,49] Removed pgRNA sequences mainly showed GU-AG (conserved boundary sequences of intron).[50] In our study, sequence comparison indicated that HBV_circ_1 has two junction sites. Junction site B was generated by deletion of the 2,986–488 nt region of the HBV genome from pgRNA/pcRNA. Dinucleotides at the first two and last two positions of the deleted sequence were GU and AG. Therefore, we suggested that the junction site B was formed by a splicing mechanism. In addition, serine/arginine-rich-splicing factor 1, splicing factor U2AF35 kDa subunit, serine/arginine-rich-splicing factor 2, and U2 small nuclear ribonucleoprotein B were identified in the precipitation complex of HBV_circ_1-proteins, further confirming that HBV_circ_1 biosynthesis was involved in splicing.

circRNAs are produced by lariat-driven circularization, intron pairing-driven circularization, resplicing-driven circularization, and RNA-binding protein-driven circularization.[51,52] Furthermore, conservative site-specific recombination is an exchange that occurs between segments possessing sequence homology residing on the same DNA molecule or on two different DNA molecules. The result of the exchange may be insertion, deletion, and inversion of DNA sequences, depending on the orientation of the two recombination sites.[53] We observed a direct repeat sequence at the 5′ and 3′ terminals of pgRNA/pcRNA by comparing it with HBV_circ_1. Only one repeat sequence was retained in the

Please cite this article in press as: Zhu et al., Hepatocellular carcinoma progression mediated by hepatitis B virus-encoded circRNA HBV_circ_1 through interaction with CDK1, Molecular Therapy: Nucleic Acids (2021), https://doi.org/10.1016/j.omtn.2021.08.011

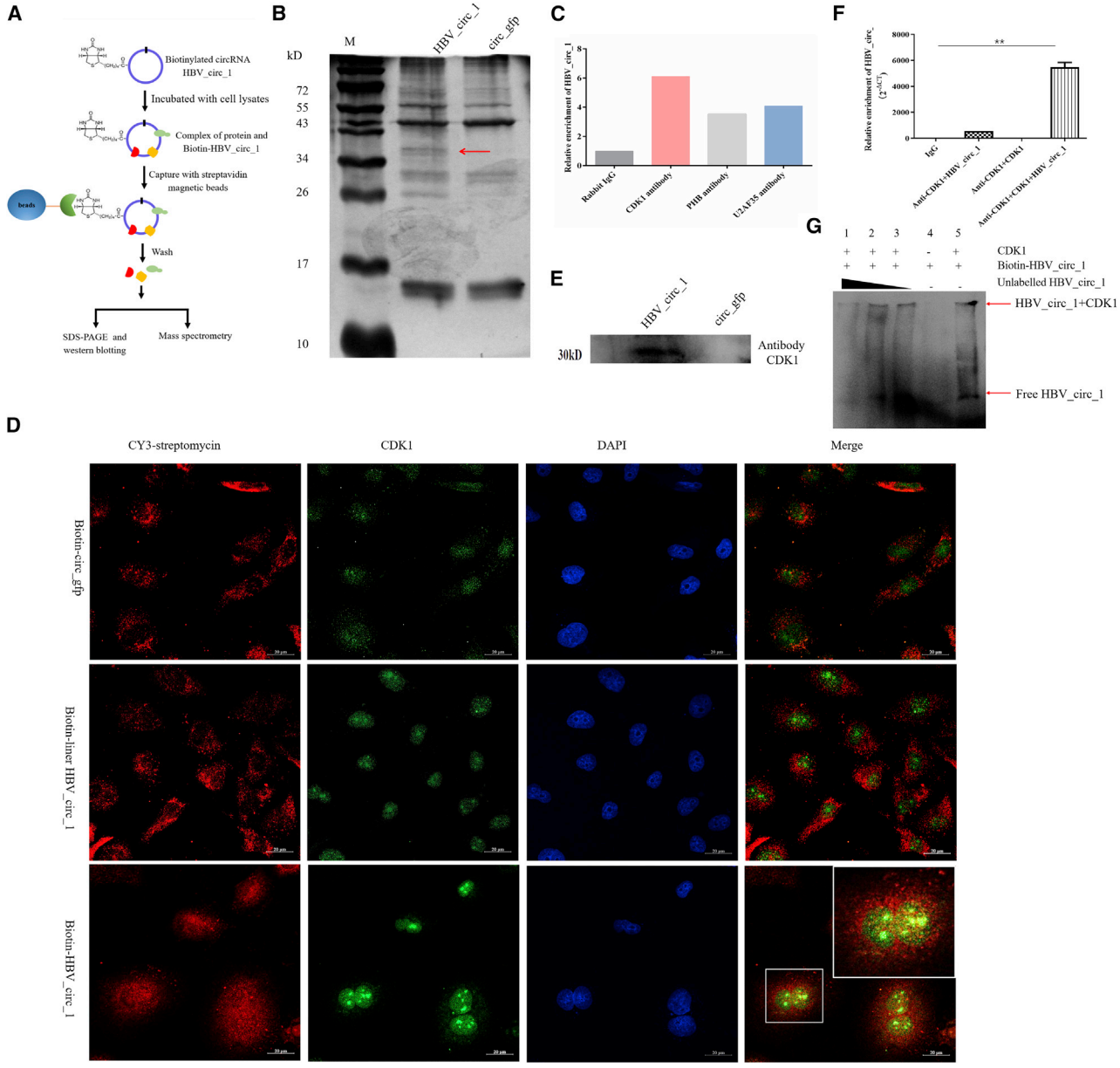

Figure 5. HBV_circ_1 regulates cell cycle by interacting with the CDK1 protein

(A) The RNA pull-down flowchart. (B) The precipitation complex of pull-down was detected by SDS polyacrylamide gel electrophoresis, and the red arrow represents a specific band. (C) RIP (RNA immunoprecipitation) experiments show that CDK1 can enrich HBV_circ_1. (D) HBV_circ_1 co-locates with CDK1. (E) CDK1 protein was detected in HBV_circ_1 pull-down complex by CDK1 antibody. (F) RIP experiment *in vitro* showed that purified recombinant CDK1 protein can enrich HBV_circ_1. (G) Binding of CDK1 to HBV_circ_1 was demonstrated by electrophoretic mobility shift assay (EMSA). Lanes 1–3: Different concentrations of unlabeled HBV_circ_1 competitively bound to CDK1 with bition-HBV_circ_1 (**p value $\leq$ 0.005).

HBV_circ_1; therefore, we suggested that HBV_circ_1 junction site A was generated by joining the two ends of pgRNA/pcRNA by conservative site-specific recombination. However, site-specific recombination events only occurred between homologous DNA. Whether homologous recombination occurs between RNA molecules remains to be elucidated.

HBV is responsible for acute and chronic hepatitis in humans, which may lead to cirrhosis or liver cancer.[54] Previous studies on the molecular mechanisms driving progression of liver cirrhosis toward hepatocellular carcinoma in chronic hepatitis B infections mainly focused on HBV DNA, RNAs, and proteins.[55] Although great progress has been made, HBV-related HCC pathogenesis remains unclear. It has

Table 2. Identification of candidate proteins interacting with HBV_circ_1 by mass spectrometry

Protein name	Pep count/unique pep count
SRSF1: HUMAN Serine/arginine-rich-splicing factor 1	11/9
PHB: HUMAN Prohibitin	8/8
RACK1: HUMAN Receptor of activated protein C kinase 1	5/5
ANXA2: HUMAN Annexin A2	4/4
U2AF35: HUMAN Splicing factor U2AF35 kDa subunit	4/4
SRSF2: HUMAN Serine/arginine-rich-splicing factor 2	3/3
CDK1: HUMAN Cyclin-dependent kinase 1	1/1
EEF1A1: HUMAN Elongation factor 1-alpha 1	1/1
CDK18: HUMAN Cyclin-dependent kinase 18	1/1
SNRPB2: HUMAN U2 small nuclear ribonucleoprotein B	1/1
ZNF26: HUMAN Zinc finger protein 26	1/1
EXOSC6: HUMAN Exosome complex component MTR3	1/1
MAPKAP1: HUMAN Target of rapamycin complex 2 subunit	1/1

been recently found that some viruses belonging to gammaherpesviruses possess functional circRNAs.[30–32] Many cellular circRNAs commonly act as miRNAs sponges. However, EBV or KSHV circRNA sequence interactions with miRNAs have not been identified. Therefore, most EBV or KSHV circRNAs were not suggested to function as miRNA sponges.[30–33] It was reported that cellular miRNAs, such as miR-122 and miR-15 family, might be sequestered by HBV pgRNA.[25,56] Whether HBV_circ_1 may function as a miRNA sponge requires further investigation.

Similar to cellular circRNAs, the intron-retained circRNAs of circRPMS1_E4_E3a and circRPMS1_E4_E2 encoded by EBV were found to be nuclear, whereas the intron-excised circRNA was located in the cytoplasm.[31] In the present study, HBV_circ_1 was shown to be nuclear and cytoplasmic. This result suggested that different distribution of HBV_circ_1 was associated with its functions. KSHV circRNAs are incorporated into KSHV virions and play a potential function in early infection.[57] Interestingly, the spliced pgRNAs may also be encapsidated and further reverse transcribed.[58,59] Whether pgRNA-derived HBV_circ_1 is incorporated into HBV virions remains to be determined.

It was reported that some circRNAs are translated into protein in a cap-independent manner. Human papillomavirus 16 (HPV 16) circRNA circE7 encodes the same E7 oncoprotein as full-length mRNA, which enhances proliferation and transformation of cancer cells.[60] The most abundant HBV pgRNA splicing variant SP1 is translated into the HBV splicing-generated protein (HBSP).[61] pgRNA-derived HBV_circ_1 has complete open reading frame of HBx. Whether HBV_circ_1 can be translated into protein deserves further investigation.

Previous studies have shown that viral circRNAs identified in the *Lymphocryptovirus* and *Rhadinovirus* genera of gammaherpesviruses function in latency and viral replication.[32] circRNA production acts in *cis* by balancing the production rates of its linear counterpart. In this study, knocking down the expression of HBV_circ_1 in HepG2.2.15 cells, the expression of HBV S gene was downregulated (data not shown). Therefore, we believe that HBV_circ_1 plays a role in latency and viral replication. Actually, HBV-encoded miRNA HBV-miR-3 controls viral replication[27] and promotes cell proliferation related to HCC development by decreasing target host protein phosphatase 1A gene expression.[62] HBV pgRNA splicing variant was found to influence cell viability, proliferation, migration, and the TNF-α signaling pathway.[63,64]

We also observed that the expression level of HBV_circ_1 in HBV-related HCCT was higher than that in paracancerous tissues. HBV_circ_1 accelerated cell proliferation and migration, inhibited apoptosis *in vitro*, increased the tumor size *in vivo*, and promoted Ki67 and cyclin D1 expression levels in the formed tumor tissue. Moreover, survival rate of HBV_circ_1-positive patients was significantly lower compared with that of HBV_circ_1-negative patients, suggesting that HBV_circ_1 contributed to HBV-related HCC progression.

At present, the evaluation of HBV activity mainly depends on HBV semi-detection and viral DNA detection. However, viral RNA may be more representative of viral activity in the host, because it is transcribed by the host system. Linear RNA is easy to degrade, which is not convenient for detection, but circRNA has a closed circular structure and is difficult to be degraded by RNA exonuclease. Therefore, HBV_circ_1 might be used as a good diagnostic and therapeutic marker to assess HBV infection and HBV-related HCC.

In addition, circRNAs may be used as protein sponges or scaffold to regulate protein activity. circ-fox3 is highly expressed in lung cancer cells and is related to the cell cycle process.[65] It is combined with CDK2 and p21 to form the circ-fox3-p21-CDK2 ternary complex to restrain CDK2 function. Loss of control of the cell cycle is an important cause of cell malignancy. Cell cycle regulation uses a histone kinase, cyclins, and CDKs. Abnormal expressions of cyclin and CDKs, or the absence of CDK inhibitory proteins, cause cell cycle disorders, leading to uncontrolled cell proliferation and eventually carcinogenesis. CDK1, also known as cell division cycle protein 2 homolog (CDC2), is a protein kinase that binds to cyclin and activates cells to cell cycle progression.[66,67] In the present study, we found that HBV_circ_1 interacted with CDK1 protein and upregulated CDK1 expression. Therefore, we suggested that HBV-related HCC development might be promoted by interaction of HBV_circ_1 with CDK1 (CDK1 is a partner of cyclin A and cyclin B).[68] However, how interaction of HBV_circ_1 with CDK1, cyclin A, and cyclin B plays a role in regulating the cell cycle remains to be further studied.

Moreover, prohibitin (PHB), CDK18, and target of rapamycin complex 2 subunit (MAPKAP1) also play important roles in apoptosis, autophagy, and cell proliferation.[69–72] In our study, these proteins were also identified in the precipitation complex of HBV_circ_1-proteins;

Please cite this article in press as: Zhu et al., Hepatocellular carcinoma progression mediated by hepatitis B virus-encoded circRNA HBV_circ_1 through interaction with CDK1, Molecular Therapy: Nucleic Acids (2021), https://doi.org/10.1016/j.omtn.2021.08.011

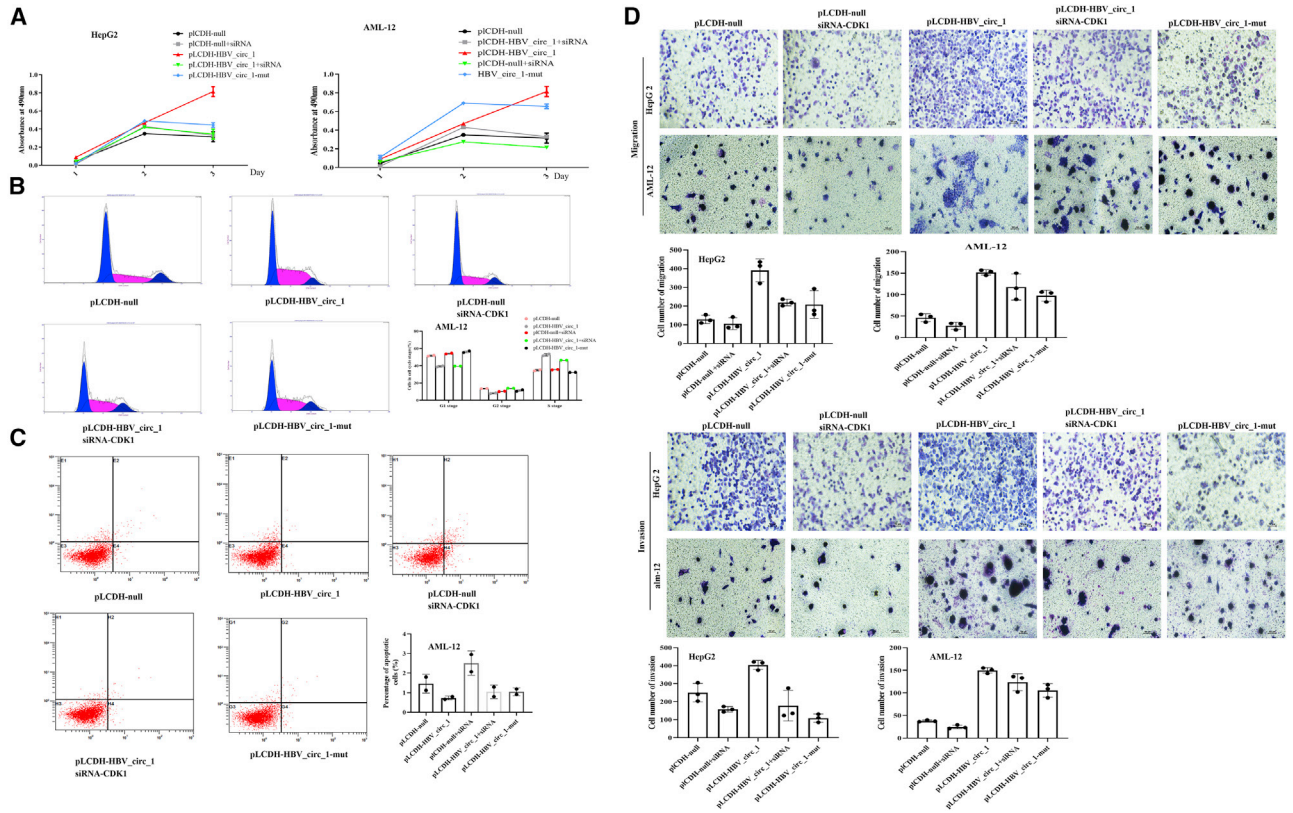

Figure 6. HBV_circ_1 stimulates cell proliferation, migration, and invasion and inhibits apoptosis by binding to CDK1

(A) Cell proliferation of the cells (HepG2 and AML-12 cell line) was determined by MTT assay. (B) Cell cycle of AML-12 was determined by flow cytometry. Results of FACS analysis were presented as the percentage of total cells. (C) Flow cytometry was used to detect the apoptosis of AML-12 cells. (D) The Transwell migration and invasion assays of the cells (HepG2 and AML-12 cell line). All tests were performed at least twice (***p value $\leq$ 0.001, **p value $\leq$ 0.005, *p value $\leq$ 0.05).

therefore, whether HBV-related HCC is promoted by interaction of HBV_circ_1 with PHB, CDK18, and MAPKAP1 remains to be investigated.

In summary, a novel circRNA HBV_circ_1 produced by HBV was identified in HepG2.2.15 cells and HBV-related HCCT. We found that HBV_circ_1 accelerated cell proliferation and migration, inhibited apoptosis *in vitro*, and increased *in vivo* tumor size. Furthermore, we confirmed that HBV_circ_1 interacted with CDK1. These results suggested that HBV-related HCC progression may be promoted by interaction of HBV_circ_1 with CDK1. Our findings provide a novel clue to understand carcinogenesis and progress of HBV-related HCC and a new target for the development of therapeutic drugs.

MATERIALS AND METHODS

Cell culture and tissue

HepG2 human liver carcinoma cell line and HBV-positive HepG2.2.15 human liver carcinoma cell line were stored in our laboratory. SMCC-7721 human liver carcinoma cell line was kindly provided by Professor Zhou at the School of Biology & Basic Medical Science, Soochow University. AML-121, a normal mouse liver cell line, was purchased from Procell Life Science & Technology (Procell, WuHan, China). All cells were maintained in DMEM/high-glucose medium (HyClone, Logan, UT, USA), containing 10% fetal calf serum (BioInd, Kibbutz Beit Haemek, Israel) in a humidified atmosphere containing 5% CO_2 at 37°C. A tissue microarray (ZH-LVC1608) was purchased from Superbiotek (http://www.superbiotek.com/productshow.asp?/1828.html) (Shanghai, China) and authorized by US Biomax (Rockville, MD, USA). We used 160 samples in the microarray, including 80 HCC tumor specimens and 80 paired paracancerous tissues.

Validation of HBV_circ_1 with Sanger sequencing

We previously conducted circRNA sequencing of the HepG 2.2.15 HBV-positive cell line using an RNase R-treated RNA library. We found a novel circRNA, assigned to HBV_circ_1, which mapped to the 489–2,985 nt region of the HBV genome (GenBank: KU668446.1). Transcript analysis of HBV showed that HBV_circ_1 has two junction sites (junction sites A and B). To validate the junction sites of HBV_circ_1 with Sanger sequencing, Primer1-Forward/Primer1-Reverse and Q-HBV_circ_1-Forward/Q-HBV_circ_1-Reverse (Table 1) were designed based on the flanking sequences of the junction sites (junction sites A and B) of HBV_circ_1 (Figure 1B). To further validate HBV_circ_1 with two junction sites, two pairs of

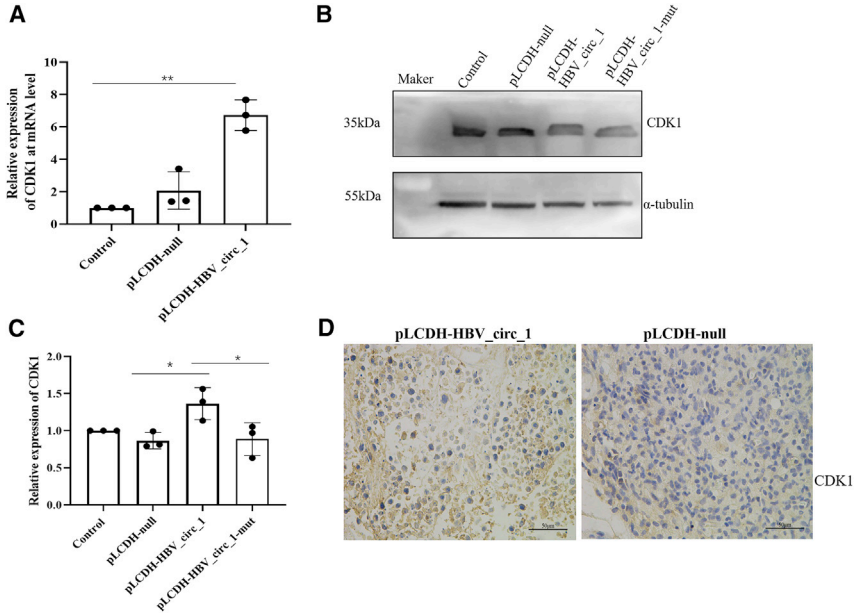

Figure 7. HBV_circ_1 regulates cell cycle by increasing CDK1 expression level

(A) The expression levels of CDK1 were detected by real-time PCR in pLCDH or pLCDH-HBV_circ_1 transfected cells, with un-transfected cells as control. This test was performed three times. (B) The expression level of CDK1 was detected by western blotting. This test was performed three times. (C) Gray value statistics for western blotting bands. (D) Representative images of immunohistochemistry that were used to detect the expression level of CDK1 in the tumor formed by SMMC-7721 cells transfected with pLCDH-HBV_circ_1 or pLCDH null. All tests were performed at least three times (**p value $\leq$ 0.01, *p value $\leq$ 0.05).

primers (Primer2-Forward and Primer3-Reverse crossing the junction site A and Primer2-Reverse and Primer3-Forward crossing the junction site B) were designed to amplify the full length of HBV_circ_1. Briefly, total RNAs were extracted using the RNAplus Kit (TaKaRa, Dalian, China), following manufacturer's instructions. After treatment with RNase R (Epicenter, Madison, WI, USA) to remove the linear RNAs, cDNAs were synthesized using the First Strand cDNA Synthesis kit (Transgene, Beijing, China) and a random hexamer from 1 μg of total RNA. Amplification of cDNA was conducted by PCR at 95°C for 5 min, 94°C for 50 s, followed by 30 cycles of annealing (temperature depending on the primer set used) for 50 s, and extension at 72°C for 30 s, with a final extension at 72°C for 10 min. PCR products were resolved on agarose gels, and recovered PCR products were directly cloned into a T-vector for Sanger sequencing.

Preparation of biotinylated circRNAs

To generate biotinylated circRNAs, *in vitro* transcription was conducted with T7 RNA polymerase (Takara, Dalian, China) and a biotin RNA labeling mix (Roche, Basel, Switzerland), using the recovered PCR product from the agarose gel as a template. The transcript product was ligated using an RNA ligase (Takara), and the ligated product was treated with DNase I and RNase R to generate biotinylated HBV_circ_1 and circ_GFP. The primer sequences T7-HBV_circ_1-Forward/ T7-HBV_circ_1-Reverse, and T7-circ_gfp-Forward/T7-circ_gfp-Reverse for *in vitro* circRNAs synthesis are listed in Table 1.

Establishment of HepG 2 cells overexpressing HBV_circ_1

To establish a HepG 2 cell line transiently overexpressing HBV_circ_1, the full length of 2,497-bp HBV_circ_1 was subcloned into a pLCDH-ciR lentiviral expression vector (Geneseed Biotech, Guangzhou, China) to generate the pLCDH-HBV_circ_1 plasmid. The full-length subcloned sequence containing the front circular frame, the back-circular frame, and full length of HBV_circ_1 were amplified, using the pLCDH-HBV_circ_1-Forward/pLCDH-HBV_circ_1-Reverse (Sangon Biotech, Shanghai, China) primer (Table 1). Cells were transiently transfected with the pLCDH-HBV_circ_1 plasmid, using Lipofectamine 3000 (Invitrogen, Camarillo, CA, USA). Cells were then harvested at 48 h post-transfection for further use. Transfected cells with the empty vector pLCDH-ciR were used as a negative control.

Northern blotting

Detected HBV_circ_1 was validated with northern blotting, using a Northern blot kit (Ambion, Austin, TX, USA), according to manufacturer's instructions. The biotin-labeled probe specific to HBV_circ_1 junction site B was synthesized by Sangon Biotech (Table 1). Total RNA (30 μg) was resolved using a 1% agarose-formaldehyde gel, then transferred to a Hybond-N+ nylon membrane (Roche, Basel, Switzerland) and hybridized with biotin-labeled DNA probes crossing junction site B. A Biotin Chromogenic Detection kit (Thermo Scientific, Waltham, MA, USA) was used to detect the biotinylated RNAs probes.

MTT assay

To assess the effect of HBV_circ_1 on cell proliferation, cells (2×10^3) transfected with pLCDH-HBV_circ_1 or pLCDH were seeded on a 96-well plate with five replicate wells and allowed to incubate for up to 6 days. After incubation, cell viability was assessed at 4 h by the tetrazolium-based MTT colorimetric assay with a CellTiter 96-well cell proliferation assay kit (Promega, Madison, WI, US), following manufacturer's instructions. Optical densities at 490 nm were then read by an enzyme labeling instrument. Results represent three replicate determinations from three independent experiments.

Flow cytometry assay for cell cycle and cellular apoptosis detection

For cell cycle detection, cells were washed, resuspended in cold phosphate-buffered saline (PBS), and incubated in ice-cold 70% ethanol

Table 3. CDK1 siRNA sequences used in this manuscript

Gene name	Sense	Anti-sense
siRNA-CDK1-127	GGGGUUCCUAGUACUGCAAU	UUGCAGUACUAGGAACCCCUU
siRNA-CDK1-168	GGAACUUCGUCAUCCAAAUUU	AUUUGGAUGACGAAGUUCCUU
siRNA-CDK1-222	GGUUAUAUCUCAUCUUUGAGU	UCAAAGAUGAGAUAUAACCUG

for 4 h. Cells were then centrifuged at 1,000 rpm for 10 min, resuspended in propidium iodide (PI) master mix (40 mg/mL PI and 100 mg/mL RNase in PBS) at a density of 5×10^4 cells/mL, and incubated at 37°C for 30 min before flow cytometry analysis. Cellular apoptosis detection was performed according to manufacturer's instructions, using an apoptosis detection kit containing Annexin V-PE/7-AA (Biodragon, Beijing, China).

Cell migration and invasion assay

For the invasion assay, the Transwell system and Matrigel (BD Biosciences, New York, NY, USA) were used, following manufacturers' instructions. In brief, 10^4 cells were seeded into the upper chambers, which were precoated with Matrigel, and cultured in serum-free DMEM. The lower compartment was filled with DMEM supplemented with 10% fetal bovine serum (FBS) as a chemoattractant. After incubation for 24 h, the cells remaining in the upper chamber were removed, and the cells at the bottom of the insert were fixed, stained with 0.5% crystal violet, and counted under a microscope (Leica, Germany). The results from three independent experiments were averaged. For the migration assay, cells were seeded into the upper chambers without a Matrigel coating. The remainder of the assay was conducted as described for the invasion assay.

Real-time PCR

cDNA was synthesized with a random hexamer, using a First Strand cDNA Synthesis kit (Transgene, Beijing, China) from 1 μg of total RNA. Real-time PCR was conducted as following: pre-denaturation at 95°C for 3 min, followed by 39 cycles of 10 s at 95°C, 30 s at 58°C, and 1 min at 60°C, according to manufacturer's instructions. Real-time PCR primers are listed in Table 1.

Western blotting

We seeded 1×10^5 cells in 6-well plates. Cells were then collected at 48 h post-transfection and lysed with radioimmunoprecipitation assay (RIPA) lysis buffer (Beyotime Biotech, Beijing, China). Twenty micrograms of proteins were electrophoresed on a SDS polyacrylamide gel and transferred to a polyvinylidene fluoride membrane (Roche). Anti-CDK1 polyclonal antibodies (GeneTex, San Antonio, TX, USA) were used, and immunoblotting with anti-β-tubulin antibody (Proteintech, Rosemount, IL, USA) was conducted to ensure equal protein loading. Signals were then measured by an enhanced chemiluminescence (ECL) western blot detection kit (Sangon Biotech).

In situ hybridization

The HBV_circ_1 probe-A (Table 1) targeting the HBV_circ_1 B site was labeled with DIG-11-dUTP by digoxin, using a Dig high primer DNA labeling kit and detection starter kit II (Roche). Hepatic tissue paraffin sections of HCC patients were treated with dewaxing and digested with protease K. Next, coverslips were hybridized in hybridization buffer (Roche) at 37°C overnight, and signals were detected using an Enhanced Sensitive ISH detection kit I (Boster, Wuhan, China). Cell nuclei were counterstained with 4′,6-diamidino-2-phenylindole (DAPI). Images were then observed under a Leica DM2000 microscope (Leica, Wetzlar, Germany).

HBV_circ_1 and CDK1 co-location

HepG2 cells were seeded in 24-well plates at 1×10^4/well and cultured for 24 h, after which they were transfected with 35 pmol biotinylated HBV_circ_1, linear HBV_circ_1, or circ_gfp. Cells were then collected at 48 h post-transfection. After washing three times with 1 × PBS, cells were fixed in 4% paraformaldehyde. For immunofluorescence staining, cells were treated with the rabbit anti-CDK1 polyclonal antibody (1:1,000), followed by CY3-conjugated anti-biotin antibodies and fluorescein isothiocyanate (FITC)-conjugated goat anti-rabbit IgG (1:200, Service Bio, Wuhan, China). After washing, cells were counterstained with DAPI (1:1,000; Beyotime) and examined under a Zeiss ISM800 fluorescence microscope (Zeiss, Jena, Germany).

RNA pull-down

RNA pull-down assays were performed according to manufacturer's instructions, using a Pierce magnetic RNA-protein pull-down kit (Thermo Fisher Scientific, Waltham, MA, USA) to screen the binding proteins of HBV_circ_1. In brief, 1×10^7 HepG 2.2.15 cells were washed in ice-cold PBS, lysed in 500 μL coimmunoprecipitation (coIP) buffer, and incubated with 25 pmol biotinylated HBV_circ_1 at room temperature for 2 h. Meanwhile, circ_gfp was incubated with cell lysate as control. Next, 50 μL of washed streptavidin C1 magnetic beads were added to each binding reaction and incubated at room temperature for 1 h. Beads were then briefly washed with coIP buffer, five times. The bound proteins in the pull-down precipitant complex were separated by SDS-polyacrylamide gel electrophoresis. Compared with circ_gfp, the specific bands in the HBV_circ_1 group were recovered for protein identification using mass spectrometry (APTBIO, Shanghai, China). Western blotting was used to confirm HBV_circ_1-binding proteins.

Prokaryotic expression and purification of CDK1

The *CDK1* cDNA sequence (GenBank: XM_005270303.3) was synthesized by Sangon Biotech. Recombinant cDNA was further cloned into *BamH* I and *Hind* III sites of pET-28a(+) (Invitrogen, Frederick, MD, USA) to generate the prokaryotic expression vector pET28-CDK1. Thereafter, vector was transformed into *Escherichia coli* BL21

(TransGen Biotech, Beijing, China) to express recombinant protein CDK1 at 25°C. The recombinant protein CDK1 was purified by Ni-column affinity chromatography (Jingcheng, Wuhan, China).

RIP

Cells (1×10^7) were washed in ice-cold PBS and lysed in 500 μL of cell lysis buffer (0.1 M KCl, 0.5% NP-40, 5 mM $MgCl_2$, and 100 mM HEPES-NaOH [pH 7.0]) for 20 min on ice. Cell lysis supernatant was then collected. Next, 50 μL of 50% slurry of protein A/G-Sepharose was added to 100 μL NT-2 buffer (150 mM NaCl, 50 mM Tris-HCl [pH 7.4]; 1 mM $MgCl_2$, 0.05% NP40, and 20 mM EDTA [pH 8.0]; and 1 mM DTT, 100 U/mL RNase inhibitors and protease inhibitors) and mixed with 2 μg of antibodies, after which mixtures were incubated at room temperature for 1 h. Pellets were then washed three times with NT-2 buffer and resuspended in 900 μL NT-2 buffer. Subsequently, 100 μL of cell lysate or purified CDK1 were added to the 900 μL mixture and incubated overnight at 4°C, after which pellets were washed five times with NT-2 buffer. The total RNA in the precipitated complex was extracted for further reverse transcription and real-time PCR to demonstrate the presence of the binding HBV_circ_1, using respective primers.

RNAi

CDK1-specific small interfering RNAs (siRNAs) (siRNA-CDK1-127, siRNA-CDK1-168, and siRNA- CDK1-222) (Table 3) were synthetized by Sangon Biotech (Shanghai, China). A total of 100 pmol of siRNA (siRNA-CDK1-127, siRNA-CDK1-168, and siRNA-CDK1-222) was transfected into HepG2 cells at the density of 2×10^6 cells per well. Cells were collected after 48 h of transfection, and total RNA and total protein were extracted. To estimate the silencing effect of respective siRNAs, CDK1 expression was determined by real-time PCR and Western blotting.

EMSA

EMSA was employed to demonstrate the binding of HBV_circ_1 and CDK1. Briefly, a binding reaction was performed in a final volume of 20 μL, containing 3 μg recombinant protein CDK1, 6 μL 50% glycerol, 2 μL 10× RNA-protein binding buffer (10 mM Tris, 1 mM EDTA, 2 M NaCl, 0.05% Tween), 0.5 pM Biotin-HBV_circ_1, with diethyl pyrocarbonate (DEPC) water added up to 20 μL, followed by incubation for 40 min at room temperature. Then, the recombinant protein binding HBV_circ_1 was run on a 6% polyacrylamide gel and transferred to a Hybond-N+ membrane (Roche, Basel, Switzerland). The membranes were dried and ultraviolet (UV)-crosslinked at 120 mJ/cm^2 using a UV-light crosslinking instrument. Then, biotin-labeled RNA was detected with the Chemiluminescent Nucleic Acid Detection Module kit (Thermo, Waltham, MA, USA). Finally, the signal was visualized by phosphorimaging (Clinx, ChemiScope 6300, Shanghai, China).

FISH using tissue microarray

Tissue microarray section slides were used for fluorescence *in situ* hybridization (FISH) with specific probes for HBV_circ_1. Slides were pre-hybridized in pre-hybridization solution at 37°C for 1 h, and hybridization was performed at 37°C overnight in a humidity chamber with hybridization solution with 6 ng/μL probe. After hybridization, slides were washed with 2× saline-sodium citrate buffer (SSC) at 37°C for 10 min, then twice with 1× SSC at 37°C for 10 min, and 0.5× SSC for 10 min. Slides were then placed in blocking buffer for 20 to 30 min at room temperature, incubated with fluorescein-avidin (1:400) for 50 min at room temperature, washed with PBS four times for 5 min, and counterstained with DAPI for 10 min. Slides were examined under a Panoramic 250-3D microscope (HISTECH, Budapest, Hungary). Each specimen was assigned a score according to the intensity of the nuclear, cytoplasmic, and membrane staining (no staining = 0; weak staining = 1; moderate staining = 2; and strong staining = 3) and the extent of stained cells (0%–5% = 0, 6%–25% = 1, 26%–50% = 2, 51%–75% = 3, and 76%–100% = 4).[73] The final immunoreactivity score was calculated by multiplying the intensity score and the proportion scores, which ranged from 0 (minimum) to 12 (maximum). Staining results were categorized into the following four types: negative (score 0; −), low (score 1–4; +), moderate (score 5–8; ++), and high (score 9–12; +++).[73] A score of 0 is negative, and those who scored 1 to 12 were positive.

Animal experiments

Twenty female BALB/c nude mice (4–6 weeks and 18–20 g) were purchased from the Laboratory Animal Center of Soochow University and bred and maintained in specific pathogen-free conditions. Mice were divided into two groups. Transfected cells with HBV_circ_1 and control SMMC-7721 cells (3×10^6 cells/mouse) in PBS were injected into the dorsal flanks of BALB/c nude mice by subcutaneous injection, respectively. Tumor volume was measured with calipers and calculated using the formula VT = 1/2(L × W× W) (VT, tumor volume; L, the maximum of tumor; W, the minimum length of tumor).[74] After 6 weeks, tumor tissues were histologically analyzed by H&E staining. Ki67, CDK1, and cyclin D1 expressing levels in tumor tissue were also detected by immunohistochemistry.

Data analysis

GraphPad Prism 6 software was used for data statistical analysis. $^*p \leq 0.05$, $^{**}p \leq 0.01$, and $^{***}p \leq 0.001$, as compared with the control group.

Ethics approval and consent to participate

The present study was approved by the Ethics Committee of Soochow University and the Ethics Committee of the First Affiliated Hospital of Soochow University.

ACKNOWLEDGMENTS

We acknowledge Prof. Yifeng Zhou of Department Biology & Basic Medical Science, Soochow University for providing SMMC-7721 cells and acknowledge EditSprings (https://www.editsprings.com/) for the expert linguistic services provided. This work was supported by the National Natural Science Foundation of China (grant nos. 31602007 and 31272500), a project funded by the Priority Academic Program of Development of Jiangsu Higher Education Institutions, graduate student scientific research innovation projects in Jiangsu province (KYCX17_2030), and the Natural Science Foundation of

the Jiangsu Higher Education Institutions of China (grant no. 19KJB320005). The funders had no role in the study design, data collection and analysis, decision to publish, or preparation of the manuscript.

AUTHOR CONTRIBUTIONS

M.Z. designed and conducted the experiments and wrote the paper. Z.L. and J.P. conducted the experiments. X.Z. conducted the statistical analyses. R.X. and G.C. participated in writing the paper. X.H. designed the experiments and wrote the paper. C.G. conceived of the study and wrote the paper. All authors read and approved the final manuscript.

DECLARATION OF INTERESTS

The authors declare no competing interests.

REFERENCES

1. Venook, A.P., Papandreou, C., Furuse, J., and de Guevara, L.L. (2010). The incidence and epidemiology of hepatocellular carcinoma: a global and regional perspective. Oncologist *15* (*Suppl 4*), 5–13.
2. Franco, E., Bagnato, B., Marino, M.G., Meleleo, C., Serino, L., and Zaratti, L. (2012). Hepatitis B: Epidemiology and prevention in developing countries. World J. Hepatol. *4*, 74–80.
3. Levrero, M., Pollicino, T., Petersen, J., Belloni, L., Raimondo, G., and Dandri, M. (2009). Control of cccDNA function in hepatitis B virus infection. J. Hepatol. *51*, 581–592.
4. Seeger, C., and Mason, W.S. (2000). Hepatitis B virus biology. Microbiol. Mol. Biol. Rev. *64*, 51–68.
5. Seeger, C., and Mason, W.S. (2015). Molecular biology of hepatitis B virus infection. Virology *479-480*, 672–686.
6. Quarleri, J. (2014). Core promoter: a critical region where the hepatitis B virus makes decisions. World J. Gastroenterol. *20*, 425–435.
7. Li, S., Qian, J., Yang, Y., Zhao, W., Dai, J., Bei, J.X., Foo, J.N., McLaren, P.J., Li, Z., Yang, J., et al. (2012). GWAS identifies novel susceptibility loci on 6p21.32 and 21q21.3 for hepatocellular carcinoma in chronic hepatitis B virus carriers. PLoS Genet. *8*, e1002791.
8. Zhang, H., Zhai, Y., Hu, Z., Wu, C., Qian, J., Jia, W., Ma, F., Huang, W., Yu, L., Yue, W., et al. (2010). Genome-wide association study identifies 1p36.22 as a new susceptibility locus for hepatocellular carcinoma in chronic hepatitis B virus carriers. Nat. Genet. *42*, 755–758.
9. Amaddeo, G., Cao, Q., Ladeiro, Y., Imbeaud, S., Nault, J.C., Jaoui, D., Gaston Mathe, Y., Laurent, C., Laurent, A., Bioulac-Sage, P., et al. (2015). Integration of tumour and viral genomic characterizations in HBV-related hepatocellular carcinomas. Gut *64*, 820–829.
10. Ura, S., Honda, M., Yamashita, T., Ueda, T., Takatori, H., Nishino, R., Sunakozaka, H., Sakai, Y., Horimoto, K., and Kaneko, S. (2009). Differential microRNA expression between hepatitis B and hepatitis C leading disease progression to hepatocellular carcinoma. Hepatology *49*, 1098–1112.
11. Zhang, X., Liu, S., Hu, T., Liu, S., He, Y., and Sun, S. (2009). Up-regulated microRNA-143 transcribed by nuclear factor kappa B enhances hepatocarcinoma metastasis by repressing fibronectin expression. Hepatology *50*, 490–499.
12. Forgues, M., Difilippantonio, M.J., Linke, S.P., Ried, T., Nagashima, K., Feden, J., Valerie, K., Fukasawa, K., and Wang, X.W. (2003). Involvement of Crm1 in hepatitis B virus X protein-induced aberrant centriole replication and abnormal mitotic spindles. Mol. Cell. Biol. *23*, 5282–5292.
13. Sung, W.K., Zheng, H., Li, S., Chen, R., Liu, X., Li, Y., Lee, N.P., Lee, W.H., Ariyaratne, P.N., Tennakoon, C., et al. (2012). Genome-wide survey of recurrent HBV integration in hepatocellular carcinoma. Nat. Genet. *44*, 765–769.
14. Chisari, F.V., Klopchin, K., Moriyama, T., Pasquinelli, C., Dunsford, H.A., Sell, S., Pinkert, C.A., Brinster, R.L., and Palmiter, R.D. (1989). Molecular pathogenesis of hepatocellular carcinoma in hepatitis B virus transgenic mice. Cell *59*, 1145–1156.
15. Terradillos, O., Billet, O., Renard, C.A., Levy, R., Molina, T., Briand, P., and Buendia, M.A. (1997). The hepatitis B virus X gene potentiates c-myc-induced liver oncogenesis in transgenic mice. Oncogene *14*, 395–404.
16. Hsieh, Y.H., Su, I.J., Wang, H.C., Tsai, J.H., Huang, Y.J., Chang, W.W., Lai, M.D., Lei, H.Y., and Huang, W. (2007). Hepatitis B virus pre-S2 mutant surface antigen induces degradation of cyclin-dependent kinase inhibitor p27Kip1 through c-Jun activation domain-binding protein 1. Mol. Cancer Res. *5*, 1063–1072.
17. Villanueva, A., Portela, A., Sayols, S., Battiston, C., Hoshida, Y., Méndez-González, J., Imbeaud, S., Letouzé, E., Hernandez-Gea, V., Cornella, H., et al.; HEPTROMIC Consortium (2015). DNA methylation-based prognosis and epidrivers in hepatocellular carcinoma. Hepatology *61*, 1945–1956.
18. Calvisi, D.F., Ladu, S., Gorden, A., Farina, M., Lee, J.S., Conner, E.A., Schroeder, I., Factor, V.M., and Thorgeirsson, S.S. (2007). Mechanistic and prognostic significance of aberrant methylation in the molecular pathogenesis of human hepatocellular carcinoma. J. Clin. Invest. *117*, 2713–2722.
19. Kojima, H., Kaita, K.D., Xu, Z., Ou, J.H., Gong, Y., Zhang, M., and Minuk, G.Y. (2003). The absence of up-regulation of telomerase activity during regeneration after partial hepatectomy in hepatitis B virus X gene transgenic mice. J. Hepatol. *39*, 262–268.
20. Wang, G., Dong, F., Xu, Z., Sharma, S., Hu, X., Chen, D., Zhang, L., Zhang, J., and Dong, Q. (2017). MicroRNA profile in HBV-induced infection and hepatocellular carcinoma. BMC Cancer *17*, 805.
21. Sartorius, K., Makarova, J., Sartorius, B., An, P., Winkler, C., Chuturgoon, A., and Kramvis, A. (2019). The Regulatory Role of MicroRNA in Hepatitis-B Virus-Associated Hepatocellular Carcinoma (HBV-HCC) Pathogenesis. Cells *8*, 1504.
22. Sadri Nahand, J., Bokharaei-Salim, F., Salmaninejad, A., Nesaei, A., Mohajeri, F., Moshtzan, A., Tabibzadeh, A., Karimzadeh, M., Moghoofei, M., Marjani, A., et al. (2019). microRNAs: Key players in virus-associated hepatocellular carcinoma. J. Cell. Physiol. *234*, 12188–12225.
23. Qiu, L., Wang, T., Xu, X., Wu, Y., Tang, Q., and Chen, K. (2017). Long Non-Coding RNAs in Hepatitis B Virus-Related Hepatocellular Carcinoma: Regulation, Functions, and Underlying Mechanisms. Int. J. Mol. Sci. *18*, 2505.
24. Sekiba, K., Otsuka, M., Ohno, M., Yamagami, M., Kishikawa, T., Suzuki, T., Ishibashi, R., Seimiya, T., Tanaka, E., and Koike, K. (2018). Hepatitis B virus pathogenesis: Fresh insights into hepatitis B virus RNA. World J. Gastroenterol. *24*, 2261–2268.
25. Li, C., Wang, Y., Wang, S., Wu, B., Hao, J., Fan, H., Ju, Y., Ding, Y., Chen, L., Chu, X., et al. (2013). Hepatitis B virus mRNA-mediated miR-122 inhibition upregulates PTTG1-binding protein, which promotes hepatocellular carcinoma tumor growth and cell invasion. J. Virol. *87*, 2193–2205.
26. Yao, L., Zhou, Y., Sui, Z., Zhang, Y., Liu, Y., Xie, H., Gao, H., Fan, H., Zhang, Y., Liu, M., et al. (2019). HBV-encoded miR-2 functions as an oncogene by downregulating TRIM35 but upregulating RAN in liver cancer cells. EBioMedicine *48*, 117–129.
27. Yang, X., Li, H., Sun, H., Fan, H., Hu, Y., Liu, M., Li, X., and Tang, H. (2017). Hepatitis B Virus-Encoded MicroRNA Controls Viral Replication. J. Virol. *91*, e01919–e01934.
28. Legnini, I., Di Timoteo, G., Rossi, F., Morlando, M., Briganti, F., Sthandier, O., Fatica, A., Santini, T., Andronache, A., Wade, M., et al. (2017). Circ-ZNF609 Is a Circular RNA that Can Be Translated and Functions in Myogenesis. Mol. Cell *66*, 22–37.e9.
29. Pamudurti, N.R., Bartok, O., Jens, M., Ashwal-Fluss, R., Stottmeister, C., Ruhe, L., Hanan, M., Wyler, E., Perez-Hernandez, D., Ramberger, E., et al. (2017). Translation of CircRNAs. Mol Cell *66*, 9–21.e7.
30. Ungerleider, N., Concha, M., Lin, Z., Roberts, C., Wang, X., Cao, S., Baddoo, M., Moss, W.N., Yu, Y., Seddon, M., et al. (2018). The Epstein Barr virus circRNAome. PLoS Pathog. *14*, e1007206.
31. Toptan, T., Abere, B., Nalesnik, M.A., Swerdlow, S.H., Ranganathan, S., Lee, N., Shair, K.H., Moore, P.S., and Chang, Y. (2018). Circular DNA tumor viruses make circular RNAs. Proc. Natl. Acad. Sci. USA *115*, E8737–E8745.
32. Ungerleider, N.A., Jain, V., Wang, Y., Maness, N.J., Blair, R.V., Alvarez, X., Midkiff, C., Kolson, D., Bai, S., Roberts, C., et al. (2019). Comparative Analysis of Gammaherpesvirus Circular RNA Repertoires: Conserved and Unique Viral Circular RNAs. J. Virol. *93*, e01952–e01969.
33. Tagawa, T., Gao, S., Koparde, V.N., Gonzalez, M., Spouge, J.L., Serquiña, A.P., Lurain, K., Ramaswami, R., Uldrick, T.S., Yarchoan, R., and Ziegelbauer, J.M. (2018).

Discovery of Kaposi's sarcoma herpesvirus-encoded circular RNAs and a human antiviral circular RNA. Proc. Natl. Acad. Sci. USA *115*, 12805–12810.

34. Huang, J.T., Chen, J.N., Gong, L.P., Bi, Y.H., Liang, J., Zhou, L., He, D., and Shao, C.K. (2019). Identification of virus-encoded circular RNA. Virology *529*, 144–151.
35. Cai, Z., Fan, Y., Zhang, Z., Lu, C., Zhu, Z., Jiang, T., Shan, T., and Peng, Y. (2020). VirusCircBase: a database of virus circular RNAs. Brief Bioinform *22*, 2182–2190.
36. Sekiba, K., Otsuka, M., Ohno, M., Kishikawa, T., Yamagami, M., Suzuki, T., Ishibashi, R., Seimiya, T., Tanaka, E., and Koike, K. (2018). DHX9 regulates production of hepatitis B virus-derived circular RNA and viral protein levels. Oncotarget *9*, 20953–20964.
37. Xiao, M.S., and Wilusz, J.E. (2019). An improved method for circular RNA purification using RNase R that efficiently removes linear RNAs containing G-quadruplexes or structured 3′ ends. Nucleic Acids Res. *47*, 8755–8769.
38. Hansen, T.B., Venø, M.T., Damgaard, C.K., and Kjems, J. (2016). Comparison of circular RNA prediction tools. Nucleic Acids Res. *44*, e58.
39. Miller, I., Min, M., Yang, C., Tian, C., Gookin, S., Carter, D., and Spencer, S.L. (2018). Ki67 is a Graded Rather than a Binary Marker of Proliferation versus Quiescence. Cell Rep. *24*, 1105–1112.e5.
40. Massagué, J. (2004). G1 cell-cycle control and cancer. Nature *432*, 298–306.
41. Adhikari, D., Zheng, W., Shen, Y., Gorre, N., Ning, Y., Halet, G., Kaldis, P., and Liu, K. (2012). Cdk1, but not Cdk2, is the sole Cdk that is essential and sufficient to drive resumption of meiosis in mouse oocytes. Hum. Mol. Genet. *21*, 2476–2484.
42. Kramer, M.C., Liang, D., Tatomer, D.C., Gold, B., March, Z.M., Cherry, S., and Wilusz, J.E. (2015). Combinatorial control of Drosophila circular RNA expression by intronic repeats, hnRNPs, and SR proteins. Genes Dev. *29*, 2168–2182.
43. Ye, C.Y., Zhang, X., Chu, Q., Liu, C., Yu, Y., Jiang, W., Zhu, Q.H., Fan, L., and Guo, L. (2017). Full-length sequence assembly reveals circular RNAs with diverse non-GT/AG splicing signals in rice. RNA Biol. *14*, 1055–1063.
44. Hu, X., Zhu, M., Zhang, X., Liu, B., Liang, Z., Huang, L., Xu, J., Yu, L., Li, K., Zar, M.S., et al. (2018). Identification and characterization of circular RNAs in the silkworm midgut following Bombyx mori cytoplasmic polyhedrosis virus infection. RNA Biol. *15*, 292–301.
45. Shen, Y., Guo, X., and Wang, W. (2017). Identification and characterization of circular RNAs in zebrafish. FEBS Lett. *591*, 213–220.
46. Xue, D., Wang, H., Chen, Y., Shen, D., Lu, J., Wang, M., Zebibula, A., Xu, L., Wu, H., Li, G., and Xia, L. (2019). Circ-AKT3 inhibits clear cell renal cell carcinoma metastasis via altering miR-296-3p/E-cadherin signals. Mol. Cancer *18*, 151.
47. Sun, X., Wang, L., Ding, J., Wang, Y., Wang, J., Zhang, X., Che, Y., Liu, Z., Zhang, X., Ye, J., et al. (2016). Integrative analysis of Arabidopsis thaliana transcriptomics reveals intuitive splicing mechanism for circular RNA. FEBS Lett. *590*, 3510–3516.
48. Sommer, G., and Heise, T. (2008). Posttranscriptional control of HBV gene expression. Front. Biosci. *13*, 5533–5547.
49. Black, D.L. (2003). Mechanisms of alternative pre-messenger RNA splicing. Annu. Rev. Biochem. *72*, 291–336.
50. Su, T.S., Lai, C.J., Huang, J.L., Lin, L.H., Yauk, Y.K., Chang, C.M., Lo, S.J., and Han, S.H. (1989). Hepatitis B virus transcript produced by RNA splicing. J. Virol. *63*, 4011–4018.
51. Xiao, M.S., Ai, Y., and Wilusz, J.E. (2020). Biogenesis and Functions of Circular RNAs Come into Focus. Trends Cell Biol. *30*, 226–240.
52. Chen, I., Chen, C.Y., and Chuang, T.J. (2015). Biogenesis, identification, and function of exonic circular RNAs. Wiley Interdiscip. Rev. RNA *6*, 563–579.
53. Grindley, N.D.F., Whiteson, K.L., and Rice, P.A. (2006). Mechanisms of site-specific recombination. Annu. Rev. Biochem. *75*, 567–605.
54. Paoli, J., Wortmann, A.C., Klein, M.G., Pereira, V.R.Z.B., Cirolini, A.M., Godoy, B.A., Fagundes, N.J.R., Wolf, J.M., Lunge, V.R., and Simon, D. (2018). HBV epidemiology and genetic diversity in an area of high prevalence of hepatitis B in southern Brazil. Braz. J. Infect. Dis. *22*, 294–304.
55. Kanda, T., Goto, T., Hirotsu, Y., Moriyama, M., and Omata, M. (2019). Molecular Mechanisms Driving Progression of Liver Cirrhosis towards Hepatocellular Carcinoma in Chronic Hepatitis B and C Infections: A Review. Int. J. Mol. Sci. *20*, 1358.
56. Wang, Y., Jiang, L., Ji, X., Yang, B., Zhang, Y., and Fu, X.D. (2013). Hepatitis B viral RNA directly mediates down-regulation of the tumor suppressor microRNA miR-15a/miR-16-1 in hepatocytes. J. Biol. Chem. *288*, 18484–18493.
57. Abere, B., Li, J., Zhou, H., Toptan, T., Moore, P.S., and Chang, Y. (2020). Kaposi's Sarcoma-Associated Herpesvirus-Encoded circRNAs Are Expressed in Infected Tumor Tissues and Are Incorporated into Virions. MBio *11*, e03027–e03045.
58. Terré, S., Petit, M.A., and Bréchot, C. (1991). Defective hepatitis B virus particles are generated by packaging and reverse transcription of spliced viral RNAs in vivo. J. Virol. *65*, 5539–5543.
59. Bayliss, J., Lim, L., Thompson, A.J., Desmond, P., Angus, P., Locarnini, S., and Revill, P.A. (2013). Hepatitis B virus splicing is enhanced prior to development of hepatocellular carcinoma. J. Hepatol. *59*, 1022–1028.
60. Zhao, J., Lee, E.E., Kim, J., Yang, R., Chamseddin, B., Ni, C., Gusho, E., Xie, Y., Chiang, C.M., Buszczak, M., et al. (2019). Transforming activity of an oncoprotein-encoding circular RNA from human papillomavirus. Nat. Commun. *10*, 2300.
61. Soussan, P., Garreau, F., Zylberberg, H., Ferray, C., Brechot, C., and Kremsdorf, D. (2000). In vivo expression of a new hepatitis B virus protein encoded by a spliced RNA. J. Clin. Invest. *105*, 55–60.
62. Chavalit, T., Nimsamer, P., Sirivassanametha, K., Anuntakarun, S., Saengchoowong, S., Tangkijvanich, P., and Payungporn, S. (2020). Hepatitis B Virus-Encoded MicroRNA (HBV-miR-3) Regulates Host Gene PPM1A Related to Hepatocellular Carcinoma. MicroRNA *9*, 232–239.
63. Bayard, F., Godon, O., Nalpas, B., Costentin, C., Zhu, R., Soussan, P., Vallet-Pichard, A., Fontaine, H., Mallet, V., Pol, S., and Michel, M.L. (2012). T-cell responses to hepatitis B splice-generated protein of hepatitis B virus and inflammatory cytokines/chemokines in chronic hepatitis B patients. ANRS study: HB EP 02 HBSP-FIBRO. J. Viral Hepat. *19*, 872–880.
64. Pol, J.G., Lekbaby, B., Redelsperger, F., Klamer, S., Mandouri, Y., Ahodantin, J., Bieche, I., Lefevre, M., Souque, P., Charneau, P., et al. (2015). Alternative splicing-regulated protein of hepatitis B virus hacks the TNF-α-stimulated signaling pathways and limits the extent of liver inflammation. FASEB J. *29*, 1879–1889.
65. Du, W.W., Yang, W., Liu, E., Yang, Z., Dhaliwal, P., and Yang, B.B. (2016). Foxo3 circular RNA retards cell cycle progression via forming ternary complexes with p21 and CDK2. Nucleic Acids Res. *44*, 2846–2858.
66. Peters, J.M. (2006). The anaphase promoting complex/cyclosome: a machine designed to destroy. Nat. Rev. Mol. Cell Biol. *7*, 644–656.
67. Barford, D. (2011). Structural insights into anaphase-promoting complex function and mechanism. Philos. Trans. R. Soc. Lond. B Biol. Sci. *366*, 3605–3624.
68. Brown, N.R., Korolchuk, S., Martin, M.P., Stanley, W.A., Moukhametzianov, R., Noble, M.E.M., and Endicott, J.A. (2015). CDK1 structures reveal conserved and unique features of the essential cell cycle CDK. Nat. Commun. *6*, 6769.
69. Wei, Y., Chiang, W.C., Sumpter, R., Jr., Mishra, P., and Levine, B. (2017). Prohibitin 2 Is an Inner Mitochondrial Membrane Mitophagy Receptor. Cell *168*, 224–238.e10.
70. Matsuda, S., Kawamoto, K., Miyamoto, K., Tsuji, A., and Yuasa, K. (2017). PCTK3/CDK18 regulates cell migration and adhesion by negatively modulating FAK activity. Sci. Rep. *7*, 45545.
71. Dema, A., Faust, D., Lazarow, K., Wippich, M., Neuenschwander, M., Zühlke, K., Geelhaar, A., Pallien, T., Hallscheidt, E., Eichhorst, J., et al. (2020). Cyclin-Dependent Kinase 18 Controls Trafficking of Aquaporin-2 and Its Abundance through Ubiquitin Ligase STUB1, Which Functions as an AKAP. Cells *9*, 673.
72. Huang, Y., Feng, G., Cai, J., Peng, Q., Yang, Z., Yan, C., Yang, L., and Wang, Z. (2020). Sin1 promotes proliferation and invasion of prostate cancer cells by modulating mTORC2-AKT and AR signaling cascades. Life Sci. *248*, 117449.
73. Xie, P., Zhang, M., He, S., Lu, K., Chen, Y., Xing, G., Lu, Y., Liu, P., Li, Y., Wang, S., et al. (2014). The covalent modifier Nedd8 is critical for the activation of Smurf1 ubiquitin ligase in tumorigenesis. Nat. Commun. *5*, 3733.
74. Xu, X., Zhang, J., Tian, Y., Gao, Y., Dong, X., Chen, W., Yuan, X., Yin, W., Xu, J., Chen, K., et al. (2020). CircRNA inhibits DNA damage repair by interacting with host gene. Mol. Cancer *19*, 128.